Periodic self-similar wave maps coupled to gravity

Piotr Bizoń and Sebastian J. Szybka
Institute of Physics, Jagellonian University, Kraków, Poland

Arthur Wasserman
Department of Mathematics, University of Michigan, Ann Arbor, Michigan, 48109-1109, USA
(Received 10 October 2003; published 17 March 2004)

We continue our studies of spherically symmetric self-similar solutions in the $SU(2)$ sigma model coupled to gravity. Using mixed numerical and analytical methods we show the existence of an unstable periodic solution lying at the boundary between the basins of two generic attractors.

DOI: 10.1103/PhysRevD.69.064014 PACS number(s): 04.20.Dw, 04.20.Ex

I. INTRODUCTION

This is the third paper in a series aimed at understanding the structure of self-similar spherically symmetric wave maps coupled to gravity. In the first two papers [1,2] we showed that for small values of the coupling constant there exists a countable family of solutions that are analytic below the Cauchy horizon of the central singularity. In this paper we wish to elaborate on the analysis of a periodic self-similar solution whose existence was only briefly mentioned in [1]. We tried to make this paper self-contained mathematically but we refer the reader to [1] for the discussion of the physical background of the problem and to [3] for more on the role of self-similar solutions in gravitational collapse.

II. SETUP

For the reader's convenience we repeat from [1] the basic setting for the problem. Let $X:M\to N$ be a map from a spacetime (M,g_{ab}) into a Riemannian manifold (N,G_{AB}). Wave maps coupled to gravity are defined as extrema of the action

$$S=\int_M\left(\frac{R}{16\pi G}-\frac{f_\pi^2}{2}g^{ab}\partial_a X^A\partial_b X^B G_{AB}\right)dv_g. \tag{1}$$

Here G is Newton's constant and f_π^2 is the wave map coupling constant. The dimensionless parameter $\alpha=4\pi G f_\pi^2$ characterizes the strength of the coupling. The field equations derived from Eq. (1) are the wave map equation

$$\Box_g X^A+\Gamma^A_{BC}(X)\partial_a X^B\partial_b X^C g^{ab}=0, \tag{2}$$

where $\Gamma^A_{BC}(X)$ are the Christoffel symbols of the target metric G_{AB} and $\Box_g$ is the d'Alembertian associated with the metric g_{ab}, and the Einstein equations $R_{ab}-1/2\,g_{ab}R=8\pi G T_{ab}$ with the stress-energy tensor

$$T_{ab}=f_\pi^2\left(\partial_a X^A\partial_b X^B-\frac{1}{2}g_{ab}(g^{cd}\partial_c X^A\partial_d X^B)\right)G_{AB}. \tag{3}$$

As a target manifold we take the three-sphere S^3 with the standard metric in polar coordinates $X^A=(F,\Theta,\Phi)$

$$G_{AB}dX^A dX^B=dF^2+\sin^2F(d\Theta^2+\sin^2\Theta\,d\Phi^2). \tag{4}$$

For the domain manifold we assume spherical symmetry and use Schwarzschild coordinates

$$g_{ab}dx^a dx^b=-e^{-2\delta}A\,dt^2+A^{-1}dr^2+r^2(d\theta^2+\sin^2\theta\,d\phi^2), \tag{5}$$

where δ and A are functions of (t,r). Next, we assume that the wave maps are corotational, that is,

$$F=F(t,r),\quad \Theta=\theta,\quad \Phi=\phi. \tag{6}$$

Equation (2) then reduces to the single semilinear wave equation

$$\Box_g F-\frac{\sin(2F)}{r^2}=0, \tag{7}$$

where

$$\Box_g=-e^{\delta}\partial_t(e^{\delta}A^{-1}\partial_t)+\frac{e^{\delta}}{r^2}\partial_r(r^2e^{-\delta}A\partial_r), \tag{8}$$

and the Einstein equations become

$$\partial_t A=-2\alpha r A(\partial_t F)(\partial_r F), \tag{9}$$

$$\partial_r\delta=-\alpha r[(\partial_r F)^2+A^{-2}e^{2\delta}(\partial_t F)^2], \tag{10}$$

$$\partial_r A=\frac{1-A}{r}-\alpha r\left(A(\partial_r F)^2+A^{-1}e^{2\delta}(\partial_t F)^2+2\frac{\sin^2F}{r^2}\right). \tag{11}$$

These equations are invariant under dilations $(t,r)\to(\lambda t,\lambda r)$ so it is natural to look for continuously self-similar solutions, that is, solutions which are left invariant by the action of the homothetic Killing vector $K=t\partial_t+r\partial_r$. Such solutions are functions of the similarity variable $\rho=r/(-t)$ only. For our purposes it is more convenient to use another independent variable x, which is related to ρ by the transformation

$$\frac{dx}{d\rho}=\frac{e^{-\delta}A}{\rho^2}. \tag{12}$$

Assuming that $A=A(x)$, $F=F(x)$, and using an auxiliary function $W(x)=e^{-\delta}A/\rho$, we showed in [1] that Eqs. (7)–(11) reduce to the following system of autonomous ordinary differential equations (where the prime indicates d/dx):

$$W'=-1+\alpha(1-W^2)F'^2, \tag{13}$$

$$A'=-2\alpha AWF'^2, \tag{14}$$

$$(AF')'=\frac{\sin(2F)}{W^2-1}, \tag{15}$$

subject to the constraint

$$1-A-2\alpha\sin^2 F+\alpha AF'^2(W^2-1)=0. \tag{16}$$

Since the system is autonomous, without loss of generality we may assume that the past light cone of the singularity is located at $x=0$. We are interested in solutions of Eqs. (13)–(16) starting at $x=0$ with the following initial conditions (as explained in [1] these conditions ensure regularity of solutions at the past light cone of the singularity):

$$F(0)=\frac{\pi}{2},\quad F'(0)=b,\quad W(0)=1,\quad A(0)=1-2\alpha, \tag{17}$$

where b is a free parameter (since the system has reflection symmetry $F\to -F$ we may take $b>0$ without loss of generality). The value $A(0)$ follows from the constraint (16). In what follows we shall refer to solutions of Eqs. (13)–(16) satisfying the initial conditions (17) as b-orbits. We showed in [2] that, for $\alpha<1/2$, b-orbits exist locally and are analytic in b and x. Throughout the paper we assume that $\alpha<1/2$.

It follows immediately from Eqs. (13)–(16) that a b-orbit can be continued as long as $|W|<1$ (since then $0<A<1$). However, if W hits ± 1 at some x, then the solution becomes singular. We showed in [1] that generic b-orbits become singular in finite time. More specifically, we showed that b-orbits tend in finite time to $W=-1$ if b is small, or to $W=+1$ if b is large. In what follows, we shall refer to these two kinds of solutions as type A and type B orbits, respectively. Now, we show that the sets of type A and type B orbits are open.

Lemma 1. If $W(x)>0$ and $A(x)<1/2-\alpha$ for some $x>0$ then the orbit is of type B, i.e., there is a finite x_0 such that $\lim_{x\to x_0}W(x)=1$. Moreover, $\lim_{x\to x_0}A(x)=0$.

Proof. Substituting Eq. (16) into Eq. (13), we get

$$W'=-2+\frac{1-2\alpha\sin^2 F}{A}>-2+\frac{1-2\alpha}{A}. \tag{18}$$

Thus, if $A(x)<1/2-\alpha$ then $W'(x)>0$ so if $W(x)>0$ then W remains positive. But then by Eq. (14) A decreases, which implies by Eq. (18) that W' remains positive (bounded away from zero in fact), and hence W must hit $+1$ in finite time. To prove the second part of the lemma, note that by Eqs. (13) and (14) we have (using the abbreviation $V=1-W^2$)

$$\left(\frac{V}{A}\right)'=\frac{2W}{A}. \tag{19}$$

Assume that $A(x_0)>0$. Then $(V/A)(x_0)=0$ and since $(V/A)(x)>0$ for $x<x_0$ we get a contradiction. Hence $A(x_0)=0$.

Corollary. Type B orbits are open.

Proof. If the b_0-orbit is of type B then $A(x,b_0)\to 0$ and $W(x,b_0)\to 1$ as $x\to x_0$; hence for x close to x_0 we have $A(x,b_0)<1/2-\alpha$ and $W(x,b_0)>0$. Thus for nearby b we also have $A(x,b)<1/2-\alpha$ and $W(x,b)>0$, which implies by Lemma 1 that the b-orbit is of type B.

Proposition 1. Type A orbits are open.

Proof. First, note that if the orbit is of type A and $W(x)\geqslant 0$ then $A(x)\geqslant 1/2-\alpha$ (since otherwise the orbit would be of type B by Lemma 1). But for $W<0$ by Eq. (14) $A'>0$; hence $A(x)>A(x_0)\geqslant 1/2-\alpha$ for $x\geqslant x_0$ where x_0 is the point at which $W(x_0)=0$. Thus, $A>1-2\alpha$ for type A orbits. Now, let the b_0-orbit be of type A and consider a nearby b-orbit. By continuity, there is a point x_1 such that $W(x_1,b)$ is close to -1, $W(x_1,b)<0$, and $A(x_1,b)$ is greater than, say, $1/2-\alpha$. First we show that such orbits have $W'(x,b)<0$ for all $x>x_1$. To see this, notice that from Eqs. (13)–(15)

$$W''=-2\alpha F'A^{-1}[\alpha AWF'^3(W^2-1)-WAF'+\sin(2F)];$$

hence at the first zero of $W'(x,b)$ after x_1 we have

$$W''|_{W'=0}=\frac{1}{AV}(4AW\pm 2\sqrt{\alpha V}\sin 2F). \tag{20}$$

The numerator is negative because $A>1/2-\alpha$ and W is close to -1, while the denominator is always positive; hence $W''<0$, which is a contradiction. Thus, $W'(x,b)<0$ and $\lim_{x\to x_1}W(x,b)$ exists (if the orbit stays in the region). Now we show that $W(x_2,b)=-1$ for any such orbit for some $x_2>x_1$. To prove this assume that $\lim_{x\to\infty}W(x)=\overline{W}\geqslant -1$. Integrating Eq. (13) we get

$$\int_{x_1}^{x}W'dx=x_1-x+\alpha\int_{x_1}^{x}VF'^2dx, \tag{21}$$

which gives a contradiction as $x\to\infty$ because the last integral in Eq. (21) is finite—to see this remember that A is bounded from below and hence $\ln(A)$ has a limit and therefore by Eq. (14) WF'^2 is integrable.

We now know that both type A and type B orbits are open, so there must be orbits that are not type A or type B, that is, orbits that stay in $W^2<1$ for all x. Call these type C orbits. We note that type C orbits are defined for all $x\geqslant 0$ since $A(x)>1/2-\alpha$ for all x.

Proposition 2. For any type C orbit we have

$$\liminf W(x)\leqslant 0\quad\text{and}\quad\limsup W(x)\geqslant 0. \tag{22}$$

Proof. Suppose that there is an x_1 such that $W(x)\leqslant -L<0$ for $x>x_1$ [this is equivalent to $\limsup W(x)<0$]. Then from Eq. (19)

$$\left(\frac{V}{A}\right)' = \frac{2W}{A} \leqslant \frac{-L}{A} \leqslant -L$$

for $x > x_1$ and hence $(V/A) < 0$ for some $x_2 > x_1$, which is a contradiction since $(V/A) \geqslant 0$ for all x.

Similarly, suppose that there is an x_1 such that $W(x) \geqslant L > 0$ for $x > x_1$ [this is equivalent to $\liminf W(x) > 0$]. From Lemma 1 we have that $A(x) > 1/2 - \alpha$ for $x > x_1$. Thus

$$\left(\frac{V}{A}\right)' = \frac{2W}{A} \geqslant 2L$$

for $x > x_1$ which is a contradiction since by Lemma 1 $(V/A) \leqslant 2/(1-2\alpha)$ for all x.

From Proposition 2 we see that type C orbits must oscillate at infinity about $W = 0$ (unless $\lim W = 0$ which we believe cannot happen).

Once we know that type *C* orbits exist we turn to their numerical construction. Numerics indicates that the structure of type *C* orbits is rather complicated for large α [4]. In this paper we restrict our attention to small values $\alpha \leqslant 0.42$, where the structure is simple; namely, for each given α there is a single critical value $b^*(\alpha)$ such that *b*-orbits tend to the attractor *A* (*B*) if $b < b^*$ ($b > b^*$) and the b^*-orbit is of type *C*. In other words, the b^*-orbit is a separatrix lying between two generic attractors *A* and *B*. In the next section we give numerical and analytical arguments that the b^*-orbit is asymptotically periodic.

III. NUMERICAL SOLUTION

A straightforward way to determine the critical value b^* is to take two values b_A and b_B leading to attractors *A* and *B*, respectively, and then fine-tune to b^* by bisection. This procedure yields a pair of *b* that are within a distance ϵ from b^* (where ϵ is limited by machine precision). Such marginally critical *b*-orbits exhibit a transient periodic behavior before eventually escaping toward $W = \pm 1$ (see Figs. 1 and 2).

This suggests that the system has an unstable periodic solution and the b^*-orbit belongs to its basin of attraction. In other words, the value b^* corresponds to the intersection of the line of initial data $(W = 1, F = 0, F' = b)$ with the two-dimensional stable manifold of the periodic solution. In fact, if we take any two points P_A and P_B in the phase space which lead to attractors *A* and *B*, respectively, and perform bisection, we obtain the same asymptotically periodic solution. This indicates that the stable manifold of the periodic solution is the boundary between the basins of attractors *A* and *B*.

Since the periodic solution is unstable and numerically it is impossible to set initial conditions exactly on the stable manifold, we cannot obtain too many cycles of the periodic solution. Although in our case this is not a serious difficulty because the positive Lyapunov exponents are not large (see Fig. 7 below), we would like to remark in passing that using the so called straddle-orbit method due to Battelino *et al.* [5] one can pursue the unstable periodic orbit in principle forever. This procedure, which can be viewed as a series of bisections, goes as follows. At the initial time we choose two points $P_A(x=0)$ and $P_B(x=0)$ which lead to different attractors *A* and *B* and perform bisection until the distance between the iterates $P_A(0)$ and $P_B(0)$ is less than a prescribed δ. Next we integrate the equations numerically starting from the current $P_A(0)$ and $P_B(0)$ until the distance between the trajectories exceeds δ. When this happens at some time *x* we stop the integration, assign the points $P_A(x)$ and $P_B(x)$ as current representatives, and repeat the bisection. Iterating this procedure, one can progressively construct a trajectory staying within a distance δ from the codimension-1 stable manifold. The numerical solutions obtained by this method are shown in Figs. 3–5.

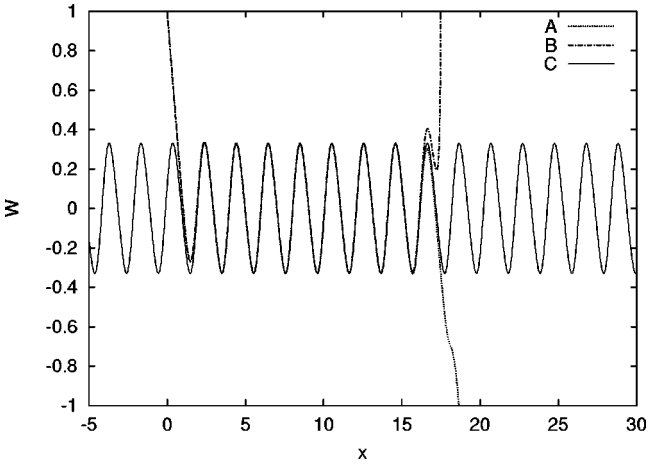

FIG. 1. The function $W(x)$ for two marginally critical *b*-orbits for $\alpha = 0.38$: the type A solution with $b = b^* - \epsilon$ (dotted line) and the type B solution with $b = b^* + \epsilon$ (dash-dotted line), where $\epsilon = 10^{-17}$. Superimposed (solid line) is the periodic solution constructed by the straddle-orbit method. See Fig. 3 in [1] for a similar plot for $\alpha = 0.2$.

Using the fact that noncritical *b*-orbits become singular in finite time, we can easily compute the positive Lyapunov exponent λ of the periodic solution. To this end, consider a marginally critical *b*-orbit with $b = b^* - \epsilon$. Such an orbit approaches the periodic solution, stays close to it for some

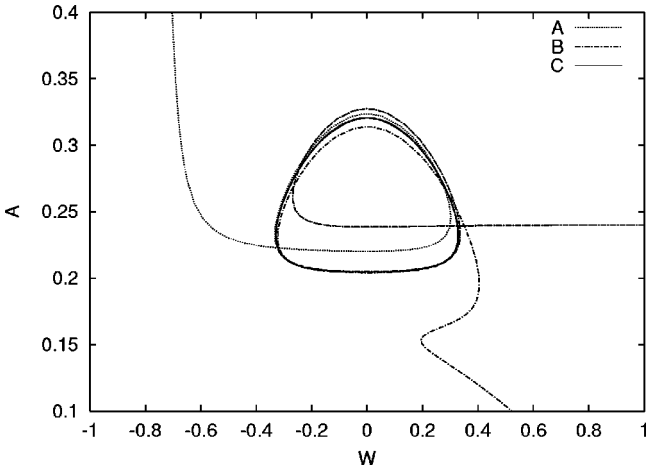

FIG. 2. The projection on the (A,W) plane of the same solution as in Fig. 1. The periodic solution is seen as the unstable limit cycle.

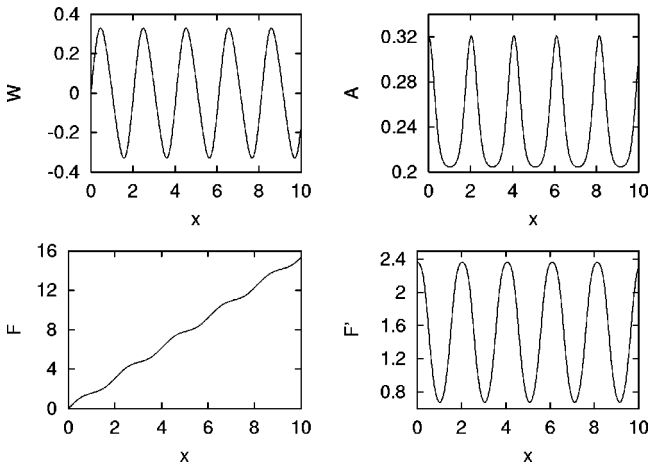

FIG. 3. The profiles of the periodic solution for $\alpha=0.38$.

time, and eventually escapes along the unstable manifold to crash at a point x_A where $W(x_A)=-1$. Therefore we can write

$$x_A = x_{\text{approach}} + x_{\text{periodic}} + x_{\text{escape}}, \tag{23}$$

where x_{approach}, x_{periodic}, and x_{escape} denote the lengths of the respective intervals of evolution (we say that the solution "escapes" if its distance from the periodic attractor exceeds a prescribed value). During the periodic interval the distance between the b-orbit with $b=b^*-\epsilon$ and the periodic solution grows at a rate proportional to $\epsilon\exp(\lambda x)$; hence $x_{\text{periodic}} \sim(-1/\lambda)\ln\epsilon$. This implies that the number of cycles n during this interval behaves as $n\sim(-1/\lambda T)\ln\epsilon$, where T is the period of the periodic solution. The length of the escape interval does not depend on the number of cycles but only on the phase of a cycle at which the escape from the periodic solution takes place; hence $x_{\text{escape}}\sim f(\ln\epsilon)$, where f is a periodic function with period λT. Summarizing, we have

$$x_A \approx -\frac{1}{\lambda}\ln\epsilon + f(\ln\epsilon) + \text{const.} \tag{24}$$

The numerical verification of this formula is shown in Fig. 6.

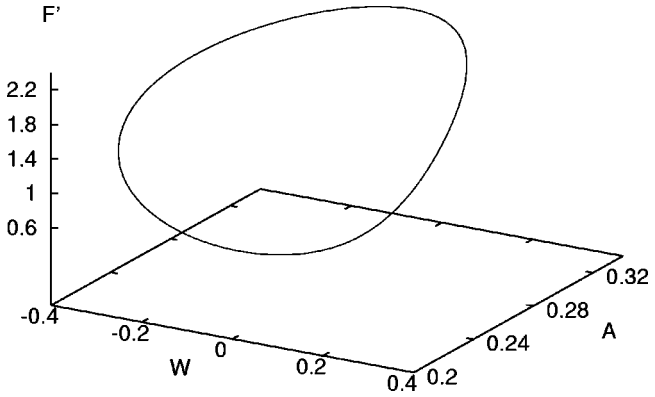

FIG. 4. The phase portrait of the periodic solution for $\alpha=0.38$.

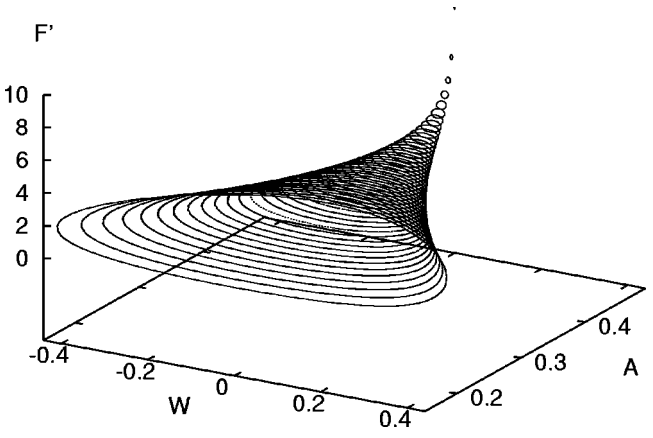

FIG. 5. The phase portraits of periodic solutions for different values of the coupling constant α ranging from 0.01 to 0.42. As $\alpha\to 0$ the loop shrinks to zero and $F'\to\infty$.

Using Eq. (24) we calculated the dependence of λ on the coupling constant α—the result is shown in Fig. 7.

IV. PERTURBATION SERIES

In order to construct periodic solutions we consider Eqs. (13)–(16) with initial conditions

$$F(0)=0, \quad F'(0)=c, \quad W(0)=0, \quad A(0)=(1+c^2)^{-1}, \tag{25}$$

where c is a free parameter and the value $A(0)$ follows from the constraint (16). We claim that for sufficiently small α there is a unique c such that $F(T)=\pi$, $F'(T)=F'(0)$, $W(T)=W(0)$, $A(T)=A(0)$ for some $T>0$. Since the system is invariant under the shift $F\to F+\pi$, we call such a solution periodic. Now we shall construct the periodic solution in a perturbative way using the Poincaré-Lindstedt method [6].

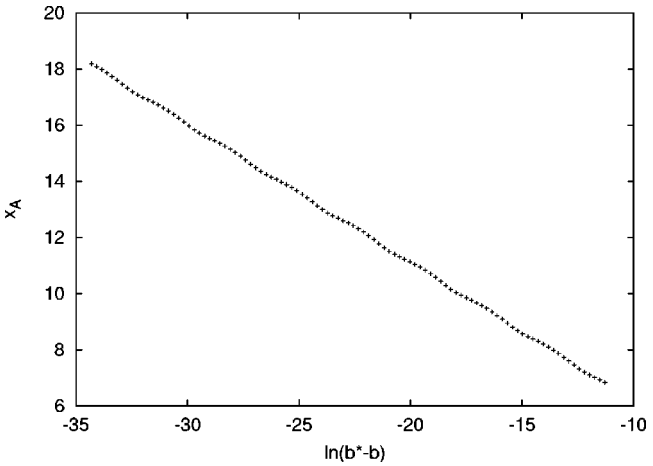

FIG. 6. For $\alpha=0.2$, the locus of the point of crash x_A is plotted as a function of the logarithmic distance from the critical value $\ln\epsilon$. The fit to the formula (24) gives $\lambda=2.029$. The period of the wiggles, corresponding to the function $f(\ln\epsilon)$, is equal to 2.887 in agreement with the predicted value λT [where $T=1.418$ was calculated independently of Eq. (35)].

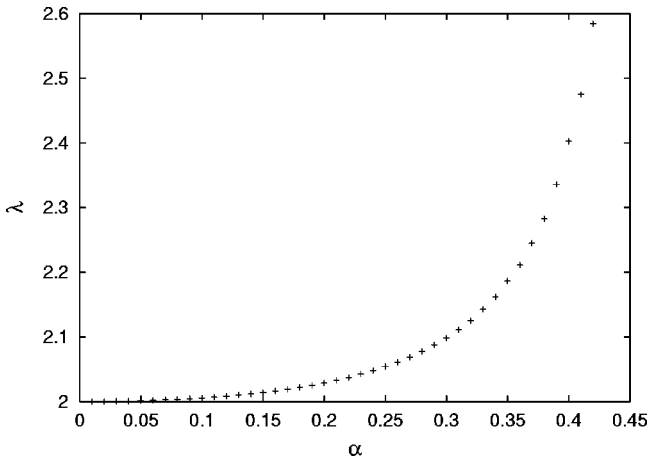

FIG. 7. The positive Lyapunov exponent λ of the periodic solution as a function of the coupling constant α.

We define the new variable $y=\omega x/\sqrt{\alpha}$ where ω is the unknown in advance frequency. We remark that the rescaling of the independent variable by $\sqrt{\alpha}$ is essential in order to have a well-defined limit for $\alpha\to 0$, while the rescaling by ω is introduced for convenience in order to have the fixed period 2π. In terms of y, Eqs. (13)–(15) transform to ($\beta=\sqrt{\alpha}$)

$$\omega W' = \beta[-1+\omega^2(1-W^2)F'^2], \tag{26}$$

$$A' = -2\omega\beta A W F'^2, \tag{27}$$

$$\omega^2(AF')' = \beta^2\frac{\sin(2F)}{W^2-1}, \tag{28}$$

and the constraint (16) becomes

$$1-A-2\beta^2\sin^2 F+\omega^2 A F'^2(W^2-1)=0. \tag{29}$$

We consider these equations on the interval $0\leqslant y\leqslant 2\pi$ with the boundary conditions

$$F(0)=0, \quad F(2\pi)=\pi, \quad W(0)=0, \quad A(0)=A_0, \tag{30}$$

where the value of the constant A_0 follows from the constraint (29). We seek solutions in the form of a power series in β:

$$W(y,\beta)=\sum_{k=0}^{\infty}\beta^k W_k(y), \quad A(y,\beta)=\sum_{k=0}^{\infty}\beta^k A_k(y),$$

$$F(y,\beta)=\sum_{k=0}^{\infty}\beta^k F_k(y). \tag{31}$$

The key idea of the Poincaré-Lindstedt method is to expand the frequency in the power series

$$\omega(\beta)=\sum_{k=0}^{\infty}\beta^k\omega_k \tag{32}$$

and to solve for the coefficients ω_k by demanding that the solution contains no secular terms. Thus, we substitute Eqs. (31) and (32) into Eqs. (26)–(29), group the terms according to powers of β, and require that the coefficients of each power of β vanish separately. In the lowest order $O(1)$ we get

$$W_0(y)=0, \quad A_0(y)=\left(1+\frac{\omega_0^2}{4}\right)^{-1}, \quad F_0(y)=\frac{y}{2}, \tag{33}$$

where ω_0 is yet undetermined. In the next order we get the equation $\omega_0 W_1'=(-1+\omega_0^2/4)$, so to avoid a secular term we need to have $\omega_0=2$. Then all $O(\beta)$ terms are zero and in the order $O(\beta^2)$ we get

$$W_2(y)=0, \quad A_2(y)=-\frac{1}{2}, \quad F_2(y)=\frac{1}{2}\sin(y). \tag{34}$$

Iterating this procedure with the help of MATHEMATICA we calculated the perturbation series up to order $O(\beta^{23})$. For example, up to order $O(\beta^8)$ we have

$$\omega(\beta)=2-\frac{\beta^4}{2}+\frac{\beta^6}{2}-\frac{49}{32}\beta^8+O(\beta^{10}), \tag{35}$$

$$W(y,\beta)=\sin(y)\beta^3+\frac{\sin(2y)}{4}\beta^5+\frac{25\sin(y)-5\sin(2y)+\sin(3y)}{16}\beta^7+O(\beta^9), \tag{36}$$

$$A(y,\beta)=\frac{1}{2}-\frac{\beta^2}{2}+\frac{-2+4\cos(y)}{8}\beta^4+\frac{-4-8\cos(y)+5\cos(2y)}{16}\beta^6 + \frac{-60+204\cos(y)-102\cos(2y)+52\cos(3y)}{384}\beta^8+O(\beta^{10}), \tag{37}$$

$$F(y,\beta)=\frac{y}{2}+\frac{\sin(y)}{2}\beta^2+16\sin(2y)\beta^4+\frac{81\sin(y)-21\sin(2y)+\sin(3y)}{96}\beta^6 + \frac{1656\sin(y)+900\sin(2y)-616\sin(3y)+9\sin(4y)}{4608}\beta^8+O(\beta^{10}). \tag{38}$$

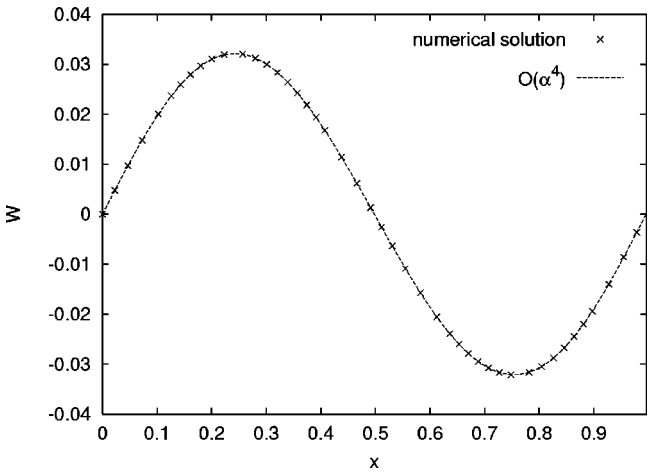

FIG. 8. For $\alpha=0.1$ we plot the numerical periodic solution and superimpose the perturbation series (35). Even at this low order the agreement is very good.

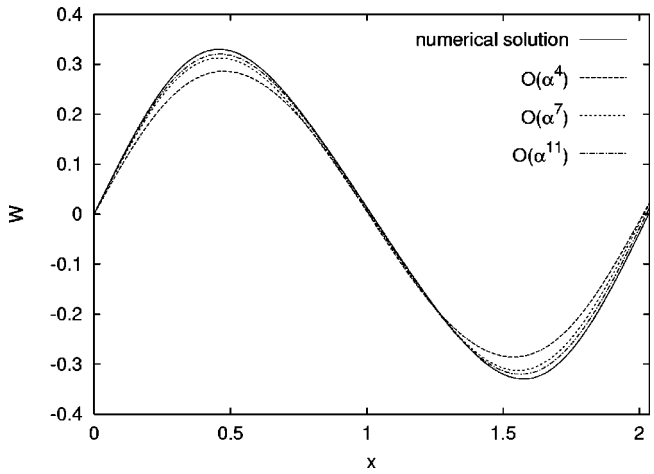

FIG. 9. For $\alpha=0.38$ we plot the numerical periodic solution and superimpose the perturbation series in different orders. As the order increases the perturbation series slowly approaches the numerical solution.

We recall that the ''physical'' frequency is equal to ω/β so it diverges as β tends to zero (while the amplitude of oscillations goes to zero). In this sense the periodic solution is nonperturbative even though we constructed it by a perturbation technique.

For small values of β the perturbation expansion converges quickly to the periodic solution constructed numerically (see Fig. 8). As β grows the convergence becomes slower and we need to take many terms in the perturbation series to approximate the numerical solution well (see Fig. 9). The fact that two independent ways of constructing the periodic solution agree makes us feel confident that the periodic solution does in fact exist.

V. FINAL REMARKS

We showed above that for small values of the coupling constant α the critical $b^*(\alpha)$-orbit is asymptotically periodic as $x\to\infty$. In previous papers [1,2] we showed that for a generic value of α, the $b^*(\alpha)$-orbit evolved backward in x becomes singular as $x\to-\infty$ (which corresponds to a singularity at the center). However, there exist isolated values of α (called α_n, $n=0,1,...$) for which the $b^*(\alpha)$-orbit is regular as $x\to-\infty$. Combining this with the result obtained above, we conclude that for a finite set of isolated values α_n (satisfying $\alpha_n<0.42$) the Einstein wave map equations admit self-similar solutions that are regular at the center and asymptotically periodic outside the past light cone.

ACKNOWLEDGMENTS

The research of P.B. and S.S. was supported in part by the KBN grant 2 P03B 006 23 and the FWF grant P15738.

[1] P. Bizoń and A. Wasserman, Phys. Rev. D **62**, 084031 (2000).
[2] P. Bizoń and A. Wasserman, Class. Quantum Grav. **19**, 3309 (2002).
[3] S. Husa, C. Lechner, M. Pürrer, J. Thornburg, and P. C. Aichelburg, Phys. Rev. D **62**, 104007 (2000).
[4] S. J. Szybka, ''Chaotic Self-Similar Wave Maps Coupled to Gravity,'' gr-qc/0310050.
[5] P. M. Battelino *et al.*, Physica D **32**, 296 (1988).
[6] R. Grimshaw, *Nonlinear Ordinary Differential Equations* (Blackwell, Oxford, 1990).